Isotopic yield and half-life of spontaneous fission for ^{284}Cn and ^{284}Fl superheavy isobars using direct calculation and semiempirical formulas

M. R. Pahlavani* and M. Joharifard†

Department of Physics, Faculty of basic science, University of Mazandaran, P.O. Box 47415-416, Babolsar, Iran

(Received 25 December 2018; published 3 April 2019)

Isotopic yields and half-lives of ^{284}Cn and ^{284}Fl superheavy nuclei are calculated using nuclear proximity and Coulomb potentials. The energy released in fission, Q value, driving potential ($V - Q$), the penetrability through barrier, fission decay constant, and relative yield for each possible pair of fission fragments are obtained. According to the fragments mass and charge asymmetry, the most favored binary fragmentation is occurred for the highest Q value and the lowest driving potential. For spontaneous binary fission of ^{284}Cn superheavy nuclei, the higher relative yields are belong to production of ^{128}Sn and ^{134}Te fragments and for ^{284}Fl superheavy isotope, the maximum yield were observed for ^{136}Xe as one of the fission fragments. The comparison between the obtained isotopic relative yield shows the role of magic and near-magic closed-shell fragments in having the highest isotopic yield. Fission decay constant for each possible fragmentation is calculated and then by summation over them, the total decay constant and fission half-life for ^{284}Cn and ^{284}Fl superheavy nuclei are estimated. Finally, the calculated half-lives using direct method are compared with the results of semiempirical formulas as well as experimental data. Satisfactory agreement is achieved between the results of this approach and the experimental data than the results of semiempirical formulas.

DOI: 10.1103/PhysRevC.99.044601

I. INTRODUCTION

One of the most complicated reactions of nuclear physics is binary fission through which a heavy or superheavy nucleus is split up into two (binary-fission) or three (ternary-fission) fragments with masses in the intermediate region. Fission reaction can occur spontaneously or induced by neutron (neutron-fission) [1,2], photon (photo-fission) [3–5], light charge particles (proton and alpha particle-fission), and accelerated ions (fusion-fission reactions) [6–10]. In recent years many experimental data are collected beside cold spontaneous binary fission of superheavy isotopes. These data contain heavy cluster decay with mass number in the range $A = 12$ to $A = 34$ [11]. Most fissions happen in the binary mode, so that in low-energy fission, a fissionable nucleus is divided in to two fission fragments after overcome to fission barrier. Fission was discovered in 1939 when Hahn and Strassman [12] discovered the presence of rare-earth elements in Uranium after irradiation by neutrons. Meitner and Frisch [13,14], shortly after discovery of fission, interpreted this phenomenon as something happening due to neutron-induced fission of Uranium. Bohr and Wheeler [15] then constructed the theory of fission on the base of nuclear liquid drop model (LDM). Due to its essential role in production of nuclear energy, fission phenomenon is studied widely both theoretically [16–18] and experimentally [19,20]. Experimental studies of cold binary fission were started by Signarbieax [21] and Armbruster [22] in the early '80s. Cold binary spontaneous fission of many actinides are measured and indicate that the most fission fragments are produced with mass numbers in the range of $A = 70$ to $A = 140$ [21–25] and several items of heavy cluster decay with zero excitation energy were also detected [26]. The first attempt to detect cold spontaneous fission was done using Ge detector to study the fissionability of ^{252}Cf isotope so that four pairs of fragments ^{104}Zr + ^{148}Ce, ^{104}Mo + ^{148}Ba, ^{106}Mo + ^{146}Ba, and ^{108}Mo + ^{144}Ba are measured [27,28]. All of these observations verified the theoretical idea of cold rearrangements of many nuclei from the ground state of the parent nuclei in to the ground state of two fragments [29,30]. Sandulescu's research group [31] and Dardenne and his collaborators [32] examined the cold spontaneous fission using GAMMASPHERE, containing 72 detectors and clearly observed the connection between the two fragments. Kumar and his collaborators [33] predicted the doubly magic ^{132}Sn isotope as one of the fission fragments of ^{252}Cf parent nucleus. Followed by this prediction, Gonnenwein and his collaborators [34] verified it experimentally. Another example of measurement of ^{132}Sn is the detection of twin-peaked shape of fragments probabilities as a function of fragments mass number for fission of Fm and Md isotopes [35], Cf and Cm isotopes form a transition area between light actinides and twin-peaked fission fragments distribution of Fm and Md parent nuclei in which the higher yields happened for fragmentations leading to produce fragments located in vicinity of doubly magic ^{132}Sn nucleus for fission of light actinides [36]. Superheavy elements with $Z = 107$–112 are produced in a cold fusion reactions between $A > 50$ beam with ^{208}Pb, and ^{209}Bi targets and with $Z = 113$–118 in hot fusion reactions between ^{40}Ca and actinide nuclei [38–42]. Smolanczuk and his colleagues [37] studied the details of even-even

*m.pahlavani@umz.ac.ir
†m.joharifard@umz.ac.ir

 ©2019 American Physical Society

superheavy nuclei located in the the range $104 \leqslant Z \leqslant 170$ using microscopic-macroscopic model in a multidimensional axial symmetric deformed space. Staszczak and his coworkers [43] estimated the fission main modes of the even-even superheavy nuclei in the ranges $108 \leqslant Z \leqslant 126$ and $148 \leqslant N \leqslant 188$ and successfully calculated the fission half-lives of these nuclei. Also, an improved model is constructed using the action integral based on the cranking inertia by Poenaru, Hoffman, and their colleagues to calculate the half-life of the spontaneous fission of superheavy nuclei, precisely [44,45]. Over the years, proximity plus coulomb potentials have been used to study α-decay, cluster radioactivity, and spontaneous fission of heavy and superheavy nuclei [46–53]. Charge and mass distribution of fission fragments and delayed-neutron yields of thermal neutron-induced fission for ^{233}U, ^{235}U, and ^{239}Pu and spontaneous fission of ^{252}Cf are evaluated using proper computer softwares [54]. In the present study, we attempt to calculate relative fission yields for different spontaneous fragmentations of ^{284}Cn and ^{284}Fl, superheavy isotopes considering Coulomb and nuclear proximity potentials. The shell effect was clearly observed for ^{72}Ni, ^{82}Ge, ^{126}Sn, ^{128}Sn, ^{134}Te, ^{136}Xe, and ^{204}Pb magic and closed-shell near magic fragments. Fission yield also increased considerably in vicinity of these fragments. Total yields and half-lives of ^{284}Cn and ^{284}Fl superheavy nuclei are also obtained.

The computational method and its formalism are defined in Sec. II. In Sec. III, the obtained results are discussed. Finally, the paper is concluded in Sec. IV.

II. EXPLANATION OF THE COMPUTATIONAL METHOD

If the Q value of a typical reaction is positive, this means that it happens spontaneously:

$$Q = M - \sum_{i=1}^{2} m_i > 0. \tag{1}$$

In this relation, M is mass excess of parent and m_i is mass excess of fragments in energy unit. Also, Q is the Q value of the reaction, which can be appear as kinetic energy of fragments.

For a superheavy nucleus undergoing spontaneous fission, the potential energy can be defined as follows:

$$V = \frac{Z_1 Z_2 e^2}{r} + V_P(s) + \frac{\hbar^2 \ell(\ell+1)}{2\,\mu\, r^2}, \quad s > 0. \tag{2}$$

Here, Z_1 and Z_2 are atomic numbers of fragments and s is the distance between near surface of two fragments. r is the center to center distance between two fragments that is related to c_1 and c_2 as central Süsmann radii of fragments with $r = s + c_1 + c_2$ [Fig. 1(b)]. Süsmann radii of fragments depend on their sharp radius, R_i, by the following relation:

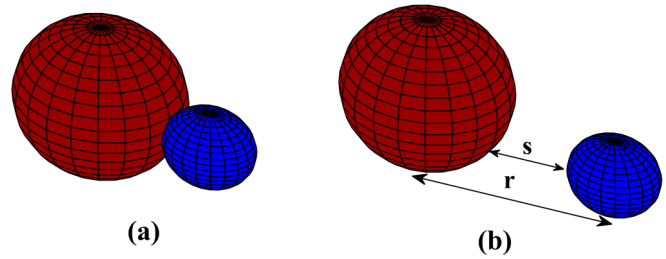

FIG. 1. (a) Diagram of the touching configuration of fission fragments ($s = 0$). (b) Diagram of the separated configuration of fission fragments ($s > 0$).

$$C_i = R_i - \left[\frac{b^2}{R_i}\right], \tag{3}$$

where b is the nuclear surface thickness parameter that is valid in the (0,1) interval. Here, b is considered to be equal to 0.86 fm.

R_i is the absolute value of fragments sharp radius that depends on their mass number through the following semiempirical relation [55]:

$$R_i = 1.28A_i^{1/3} - 0.76 + 0.8A_i^{-1/3}. \tag{4}$$

In Eq. (2), ℓ is the angular momentum and $\mu = \frac{mA_1A_2}{A_1+A_2}$ is the reduce mass of fragments with m as the average mass of nucleon.

V_P is the nuclear proximity potential that is defined as follows [55,56]:

$$V_P(s) = 4\pi\gamma b\left[\frac{c_1 c_2}{c_1 + c_2}\right]\Phi(\varepsilon), \quad \left(\varepsilon = \frac{s}{b}\right). \tag{5}$$

Where γ is the nuclear surface tension and can be evaluate using the following relation [57]:

$$\gamma = 0.9517\left[1 - 1.7826\frac{(N-Z)^2}{A^2}\right]\ \text{MeV fm}^{-2} \tag{6}$$

Here, N, Z, and A are neutron, atomic, and mass numbers of fissioning nucleus, respectively. The universal function of the proximity potential, Φ depends only on the distance between two interacting fragments [56],

$$\Phi(\varepsilon) = \begin{cases} -1.7817 + 0.9270 + 0.0169\varepsilon^2 - 0.0514\varepsilon^3 & \text{for} \quad 0 \leqslant \varepsilon \leqslant 1.9475, \\ -4.41\exp(-\varepsilon/0.7176) & \text{for} \quad \varepsilon \geqslant 1.9475, \end{cases} \tag{7}$$

where $\varepsilon = \frac{s}{b}$. Using one-dimensional WKB approximation, the tunneling probability through fission barrier is obtained as follows:

$$P = \exp\left\{-\frac{2}{\hbar}\int_{s_1}^{S_2}\sqrt{2\mu(V-Q)}ds\right\}. \tag{8}$$

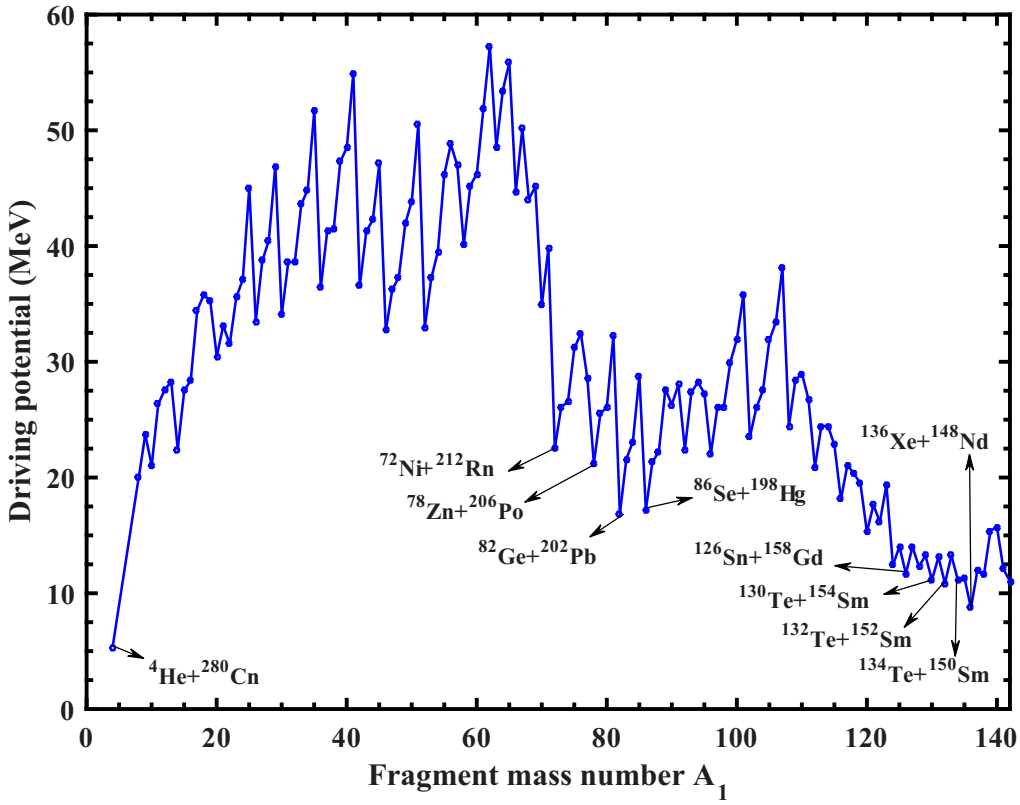

FIG. 2. Driving potential for binary spontaneous fragmentations of ^{284}Fl superheavy nucleus as a function of first fragment mass number, A_1.

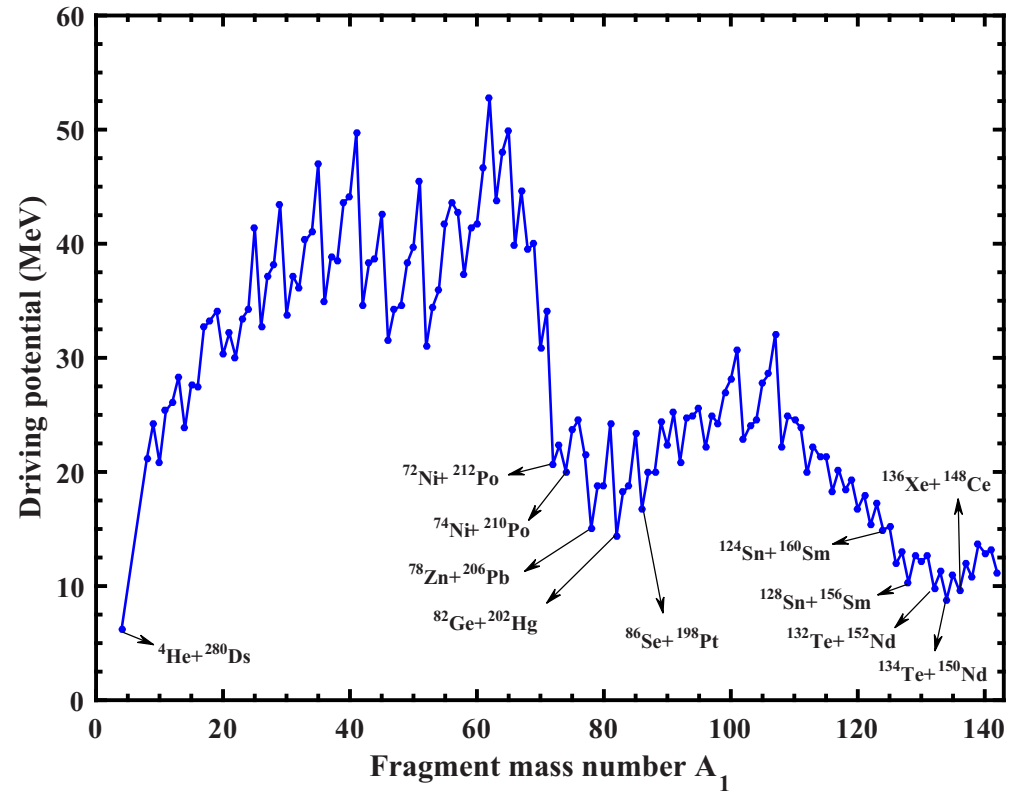

FIG. 3. Driving potential for binary spontaneous fragmentations of ^{284}Cn superheavy nucleus as a function of first fragment mass number, A_1.

TABLE I. Q values, driving potentials ($V - Q$), and relative yields of even mass fragmentation for the spontaneous fission of the ^{284}Fl superheavy isotope (yields less than 10^{-7} are ignored and substituted by "0").

A_1	A_2	Q(MeV)	V-Q(MeV)	Yield (%)	A_1	A_2	Q(MeV)	V-Q(MeV)	Yield (%)
^{4}He	^{280}Cn	10.795	5.36304	0	^{76}Ni	^{208}Rn	220.206	32.45004	0
^{8}Be	^{276}Ds	21.438	19.9798	0	^{78}Zn	^{206}Po	244.5922	21.20123	0
^{10}Be	^{274}Ds	17.1125	21.03991	0	^{80}Zn	^{204}Po	238.9096	26.09612	0
^{12}Be	^{272}Ds	7.8222	27.58604	0	^{82}Ge	^{202}Pb	260.2761	16.87036	8.19×10^{-6}
^{14}C	^{270}Hs	40.7901	22.45089	0	^{84}Ge	^{200}pb	253.319	23.08821	0
^{16}C	^{268}Hs	32.396	28.41262	0	^{86}Se	^{198}Hg	270.3772	17.18627	1.15×10^{-5}
^{18}C	^{266}Hs	22.86	35.78401	0	^{88}Se	^{196}Hg	264.63	22.24332	0
^{20}O	^{264}Sg	54.3438	30.47257	0	^{90}Se	^{194}Hg	259.904	26.31214	0
^{22}O	^{262}Sg	51.27	31.53214	0	^{92}Kr	^{192}Pt	273.9783	22.437	0
^{24}O	^{260}Sg	43.872	37.08872	0	^{94}Kr	^{190}Pt	267.575	28.23147	0
^{26}Ne	^{258}Rf	72.099	33.5147	0	^{96}Sr	^{188}Os	282.981	22.06205	0
^{28}Ne	^{256}Rf	63.398	40.46761	0	^{98}Sr	^{186}Os	278.342	26.14108	0
^{30}Mg	^{254}No	93.081	34.07442	0	^{100}Sr	^{184}Os	271.994	31.9589	0
^{32}Mg	^{252}No	86.878	38.61442	0	^{102}Zr	^{182}W	288.754	23.50052	0
^{34}Mg	^{250}No	79.037	44.90063	0	^{104}Zr	^{180}W	284.28	27.49271	0
^{36}Si	^{248}Fm	109.462	36.44374	0	^{106}Zr	^{178}W	277.877	33.44216	0
^{38}Si	^{246}Fm	102.901	41.51638	0	^{108}Mo	^{176}Hf	294.252	24.44322	0
^{40}Si	^{244}Fm	94.52	48.49528	0	^{110}Mo	^{174}Hf	289.308	28.98173	0
^{42}S	^{242}Cf	127.1707	36.56395	0	^{112}Ru	^{172}Yb	303.806	20.92076	3.63×10^{-7}
^{44}S	^{240}Cf	120.133	42.25591	0	^{114}Ru	^{170}Yb	299.906	24.46376	0
^{46}Ar	^{238}Cm	149.2479	32.68508	0	^{116}Pd	^{168}Er	311.743	18.12976	2.78×10^{-5}
^{48}Ar	^{236}Cm	143.345	37.29899	0	^{118}Pd	^{166}Er	309.2347	20.32988	9.89×10^{-7}
^{50}Ar	^{234}Cm	135.525	43.8952	0	^{120}Cd	^{164}Dy	318.845	15.29279	2.35×10^{-3}
^{52}Ca	^{232}Pu	164.8233	32.99354	0	^{122}Cd	^{162}Dy	317.7144	16.16428	5.52×10^{-4}
^{54}Ca	^{230}Pu	157.146	39.4988	0	^{124}Sn	^{160}Gd	325.0962	12.42939	2.19×10^{-1}
^{56}Ca	^{228}Pu	146.733	48.79584	0	^{126}Sn	^{158}Gd	325.625	11.69074	5.98×10^{-1}
^{58}Ti	^{226}U	172.701	40.1178	0	^{128}Sn	^{156}Gd	324.817	12.31414	2.05×10^{-1}
^{60}Ti	^{224}U	165.528	46.2235	0	**^{130}Te**	**^{154}Sm**	**328.728**	**11.15066**	**1.71**
^{62}V	^{222}Pa	162.24	57.23761	0	**^{132}Te**	**^{152}Sm**	**328.871**	**10.87218**	**2.43**
^{64}V	^{220}Pa	165.02	53.46268	0	**^{134}Te**	**^{150}Sm**	**328.5047**	**11.12784**	**1.53**
^{66}Cr	^{218}Th	181.273	44.70642	0	**^{136}Xe**	**^{148}Nd**	**332.7572**	**8.72617**	**87.6**
^{68}Mn	^{216}Ac	189.156	44.07027	0	^{138}Xe	^{146}Nd	329.8182	11.60363	8.83×10^{-1}
^{70}Fe	^{214}Ra	205.337	34.8887	0	^{140}Xe	^{144}Nd	325.6545	15.73043	1.72×10^{-3}
^{72}Ni	^{212}Rn	231.8061	22.55999	0	**^{142}Ba**	**^{142}Ce**	**331.295**	**11.0458**	**2.34**
^{74}Ni	^{210}Rn	226.985	26.50643	0					

Lower limit of integration corresponds to touching configuration of fission fragments [Fig. 1(a)] with $s_1 = 0$, and upper limit s_2 is obtained with $V(s_2) = Q$. Fission half-life, $T_{1/2}$, is obtained using the following relation:

$$T_{\frac{1}{2}} = \frac{\ln 2}{\lambda} = \frac{\ln 2}{\nu P}$$
$$(\lambda = \lambda_1 + \lambda_2 + \cdots + \lambda_n), \tag{9}$$

Where λ is the total fission decay constant that is obtained by summation over decay constants of all possible fragmentations. Also, P is the tunneling probability and $\nu = \frac{\omega}{2\pi} = \frac{2E}{h}$ is the crossing frequency of a nascent fragment with the oscillation energy E in the barrier or number of collisions through barrier in a second [58]:

$$E_\nu = Q\left\{0.056 + 0.039\exp\left[\frac{(4 - A_2)}{2.5}\right]\right\} \quad \text{for } A \geqslant 4. \tag{10}$$

Relative yield is defined as the ratio of tunneling probability of ith fragmentation to the tunneling probabilities of all possible fragment combinations,

$$Y(A_i, Z_i) = \frac{P(A_i, Z_i)}{\sum P(A_i, Z_i)}. \tag{11}$$

For each suitable fragmentation, the Q value, the driving potential, the tunneling probability, and the relative yield are evaluated. This information is used to evaluate spontaneous fission half-lives of ^{284}Fl and ^{284}Cn superheavy nuclei.

III. RESULTS AND DISCUSSIONS

Using standard evaluated mass [59–63], Q value, and driving potential ($V - Q$) for each individual fragmentation of ^{284}Fl and ^{284}Cn, superheavy nuclei are evaluated considering potential energy (V) consists of the Coulomb and the nuclear proximity potentials. For each selected fragmentation, the driving potential of ^{284}Fl and ^{284}Cn superheavy nuclei and

TABLE II. Q values, driving potentials ($V - Q$), and relative yields of even mass fragmentations for the spontaneous fission of the ^{284}Cn superheavy isotope (yields less than 10^{-7} are ignored and substituted by "0").

A_1	A_2	Q(MeV)	V-Q(MeV)	Yield (%)	A_1	A_2	Q(MeV)	V-Q(MeV)	Yield (%)
^{4}He	^{280}Ds	9.596	6.13891	0	^{76}Ni	^{208}Po	221.65	24.5486	0
^{8}Be	^{276}Hs	19.318	21.1639	0	**^{78}Zn**	**^{206}Pb**	**243.8192**	**15.0351**	**5.03×10^{-5}**
^{10}Be	^{274}Hs	16.4525	20.8086	0	^{80}Zn	^{204}Pb	239.3086	18.7741	1.54×10^{-7}
^{12}Be	^{272}Hs	8.4622	26.0921	0	**^{82}Ge**	**^{202}Hg**	**255.3101**	**14.4329**	**2.69×10^{-4}**
^{14}C	^{270}Sg	38.0401	23.7985	0	^{84}Ge	^{200}Hg	250.201	18.8184	3.32×10^{-7}
^{16}C	^{268}Sg	32.056	27.3853	0	^{86}Se	^{198}Pt	262.9572	16.7391	2.17×10^{-5}
^{18}C	^{266}Sg	24.01	33.2979	0	^{88}Se	^{196}Pt	259.079	19.942	1.51×10^{-7}
^{20}O	^{264}Rf	52.6738	30.2721	0	^{90}Se	^{194}Pt	256.11	22.268	0
^{22}O	^{262}Rf	50.88	30.0821	0	^{92}Kr	^{192}Os	267.2013	20.8974	0
^{24}O	^{260}Rf	44.9	34.2484	0	^{94}Kr	^{190}Os	262.606	24.8973	0
^{26}Ne	^{258}No	70.589	32.689	0	^{96}Sr	^{188}W	274.142	22.12	0
^{28}Ne	^{256}No	63.428	38.1293	0	^{98}Sr	^{186}W	271.482	24.2328	0
^{30}Mg	^{254}Fm	90.531	33.7999	0	^{100}Sr	^{184}W	267.076	28.1206	0
^{32}Mg	^{252}Fm	86.563	36.1318	0	^{102}Zr	^{182}Hf	280.188	22.8326	0
^{34}Mg	^{250}Fm	80.155	41.0102	0	^{104}Zr	^{180}Hf	278.053	24.4971	0
^{36}Si	^{248}Cf	107.752	34.8724	0	^{106}Zr	^{178}Hf	273.535	28.5721	0
^{38}Si	^{246}Cf	102.63	38.5309	0	^{108}Mo	^{176}Yb	286.797	22.2085	0
^{40}Si	^{244}Cf	95.642	44.1402	0	^{110}Mo	^{174}Yb	284.038	24.5717	0
^{42}S	^{242}Cm	125.3837	34.6151	0	^{112}Ru	^{172}Er	294.665	19.904	1.10×10^{-6}
^{44}S	^{240}Cm	120.03	38.6461	0	^{114}Ru	^{170}Er	292.881	21.3398	1.11×10^{-7}
^{46}Ar	^{238}Pu	146.1599	31.5617	0	^{116}Pd	^{168}Dy	300.942	18.3038	1.52×10^{-5}
^{48}Ar	^{236}Pu	141.928	34.5273	0	^{118}Pd	^{166}Dy	300.5237	18.4218	1.03×10^{-5}
^{50}Ar	^{234}Pu	135.53	39.7231	0	^{120}Cd	^{164}Gd	306.277	16.7633	1.85×10^{-4}
^{52}Ca	^{232}U	162.2063	30.9492	0	^{122}Cd	^{162}Gd	307.4424	15.3455	1.25×10^{-3}
^{54}Ca	^{230}U	156.095	35.9097	0	^{124}Sn	^{160}Sm	311.0192	14.9367	3.32×10^{-3}
^{56}Ca	^{228}U	147.228	43.6809	0	^{126}Sn	^{158}Sm	313.815	11.9367	2.77×10^{-1}
^{58}Ti	^{226}Th	170.462	37.2463	0	**^{128}Sn**	**^{156}Sm**	**315.272**	**10.3**	**32.5**
^{60}Ti	^{224}Th	164.886	41.7748	0	^{130}Te	^{154}Nd	315.723	12.1163	2.44×10^{-1}
^{62}V	^{222}Ac	161.409	52.7434	0	**^{132}Te**	**^{152}Nd**	**317.887**	**9.82059**	**8.41**
^{64}V	^{220}Ac	165.126	48.0502	0	**^{134}Te**	**^{150}Nd**	**318.7637**	**8.83631**	**39.1**
^{66}Cr	^{218}Ra	180.619	39.8196	0	**^{136}Xe**	**^{148}Ce**	**319.3772**	**9.59183**	**13.4**
^{68}Mn	^{216}Fr	187.959	39.4926	0	**^{138}Xe**	**^{146}Ce**	**318.1572**	**10.752**	**2.02**
^{70}Fe	^{214}Rn	203.38	30.8375	0	^{140}Xe	^{144}Ce	315.9685	12.9049	6.86×10^{-2}
^{72}Ni	^{212}Po	227.1461	20.7283	0	**^{142}Ba**	**^{142}Ba**	**318.234**	**11.1115**	**1.19**
^{74}Ni	^{210}Po	226.963	20.0543	0					

two fragments with mass numbers A_1 and A_2 is evaluated as a function of mass $\eta_A = \frac{A_1 - A_2}{A}$ and charge $\eta_Z = \frac{Z_1 - Z_2}{Z}$ asymmetry in touching configuration. It should be noted that for each pair of fragments with mass numbers A_1 and A_2 a pair of Z exists in which is made the driving potential minimum.

A. Driving potential ($V - Q$)

Obtained results of driving potential ($V - Q$) as a function of first fragment mass number A_1 for ^{284}Fl and ^{284}Cn superheavy nuclei are shown in Figs. 2 and 3, respectively. Due to the shell effects on one or both fragments, the minima and the mass asymmetric valley are obvious in these figures. Combination of two fission fragments regarding minima of driving potential took place with the highest probability. As one can see from Fig. 2 for driving potential of ^{284}Fl superheavy isotope, the deepest minimum belongs to ^{4}He + ^{280}Cn fragmentation. In the binary spontaneous fission of ^{284}Fl, all minima correspond to double magic, magic, or closed-shell near-magic fragments combination, which is due to shell effects. In this regard, fragmentation of ^{82}Ge + ^{202}Pb happened with high probability due to the presence of neutron magic shell, $N = 50$ and proton magic shell, $Z = 82$ for fragments ^{82}Ge and ^{202}Pb, respectively. Other combinations with minima in driving potential are ^{72}Ni + ^{212}Rn, ^{78}Zn + ^{206}Po, and ^{86}Se + ^{198}Hg, due to production of ^{72}Ni and ^{212}Rn isotopes with magic shells $Z = 82$ and $N = 126$, respectively. In the second region of fragmentation, isotope ^{126}Sn with magic shell $Z = 50$ and ^{132}Te with near-magic closed shells $Z = 52$ and $N = 80$ as in the fragmentation ^{132}Te + ^{152}Sm are highlighted. Also, the isotope ^{134}Te with magic shell $N = 82$ which is produced in the fragmentation ^{134}Te + ^{150}Sm and the magic isotope ^{136}Xe with neutron magic shell at $N = 82$ and proton near-magic closed shell at $Z = 54$ made in the fragmentation ^{136}Xe + ^{148}Nd with high probability.

Driving potential for all possible fragmentations of ^{284}Cn superheavy nucleus as a function of first fragment mass

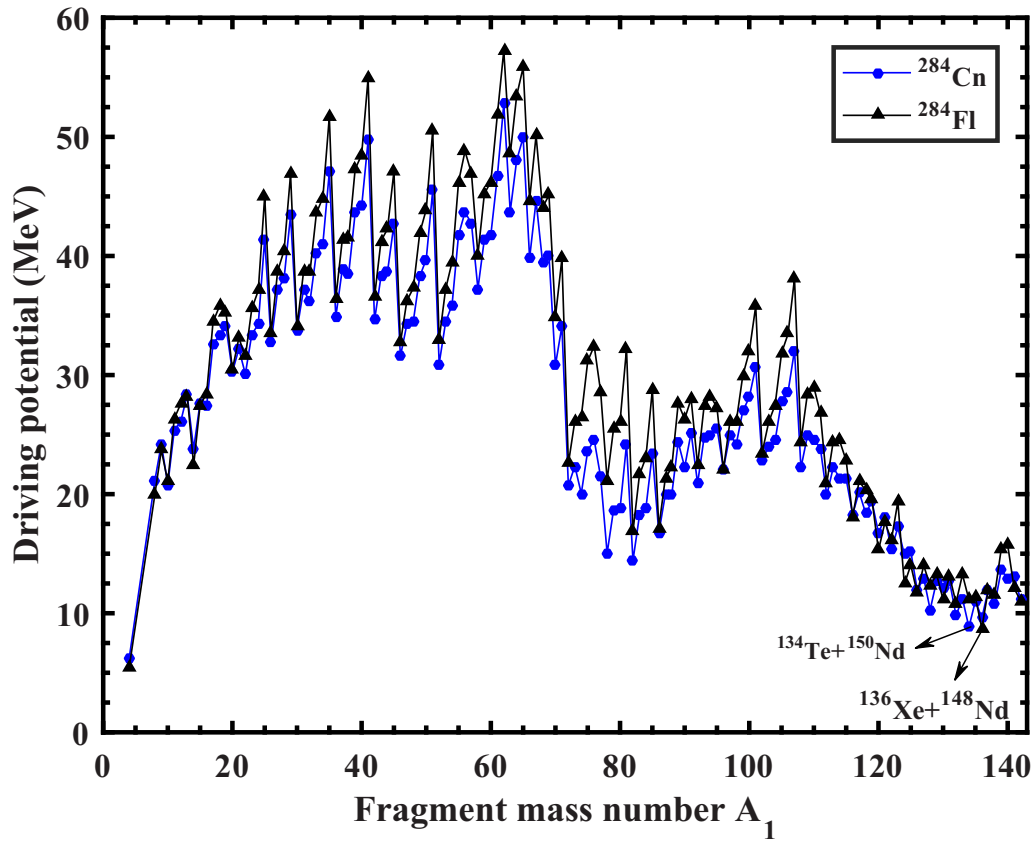

FIG. 4. The driving potential for all possible fragmentations of ^{284}Fl and ^{284}Cn superheavy nuclei as a function of first fragment mass number, A_1, are compared. The fragment combinations with the higher yield are labeled.

number, A_1, are shown in Fig. 3. The first minimum of driving potential corresponds to ^{4}He + ^{280}Ds fragmentation that is the deepest minimum of the driving potential. As it is clear in this figure, two regions of minima are obvious. In the first region, fragmentations ^{82}Ge + ^{202}Hg, ^{78}Zn + ^{206}Pb, ^{86}Se + ^{198}Pt, ^{74}Ni + ^{210}Po, and ^{72}Ni + ^{212}Po and in the second region fragmentations containing isotopes ^{124,128}Sn, ^{132,134}Te, and ^{136}Xe as one of the fragments that consist of magic or near-magic closed shell took place with high probabilities. Q values and driving potentials for all possible fragmentations are listed in Tables I and II for spontaneous fission of ^{284}Fl and ^{284}Cn superheavy isobars, respectively. Also, driving potential for ^{284}Fl and ^{284}Cn superheavy isobars are compared together in Fig. 4.

B. Penetration probability and relative yield

The penetration probability and relative yield for each fragmentation are obtained using Eqs. (8) and (11). Relative yields as a function of fission fragments mass numbers A_1 and A_2 for spontaneous fission of ^{284}Fl and ^{284}Cn superheavy nuclei are shown in Figs. 5 and 6, respectively. As is evident from Fig. 5, in spontaneous fission of ^{284}Fl superheavy nuclei, fragmentation ^{136}Xe + ^{148}Nd has the most relative yield due to the presence of fragment ^{136}Xe with $Z = 54$, proton near magic closed shell and $N = 82$, neutron magic shell. The next two fragmentations with higher relative yields are ^{132}Te + ^{152}Sm and ^{130}Te + ^{154}Sm due to the presence of isotope Te with near-double-magic closed-shells.

As is clear from Fig. 6, in spontaneous fission of ^{284}Cn superheavy isotope, fragmentation ^{134}Te + ^{150}Nd has the highest relative yield because it contains the near double magic closed-shell isotope ^{134}Te and ^{128}Sn + ^{156}Sm with proton magic shell of fragment ^{128}Sn. Fragmentations ^{136}Xe + ^{148}Ce, ^{132}Te + ^{152}Nd, and ^{138}Xe + ^{146}Ce stand in the next steps of higher relative yields due to the presence of ^{136}Xe and ^{132}Te near double magic closed-shell isotopes.

Also, the relative yields of ^{284}Fl and ^{284}Cn superheavy isobars are compared in Fig. 7. As is expected, the variations of relative yields with fragment mass number are approximately similar for these isobars.

To compare the fission relative yields for the production of odd and even mass fragments, the obtained results for odd and even mass fragments are presented by bar graph in Figs. 8 and 9 for ^{284}Fl and ^{284}Cn superheavy isobars, respectively. These figures clearly indicate the fact that the production of even mass fragments are prefer to odd mass fragments in spontaneous fission of superheavy nuclei.

C. Spontaneous fission half-lives of ^{284}Cn and ^{284}Fl superheavy isobars

The total fission decay constant is obtained by summation of the individual fragmentation decay constant λ_i, i.e.,

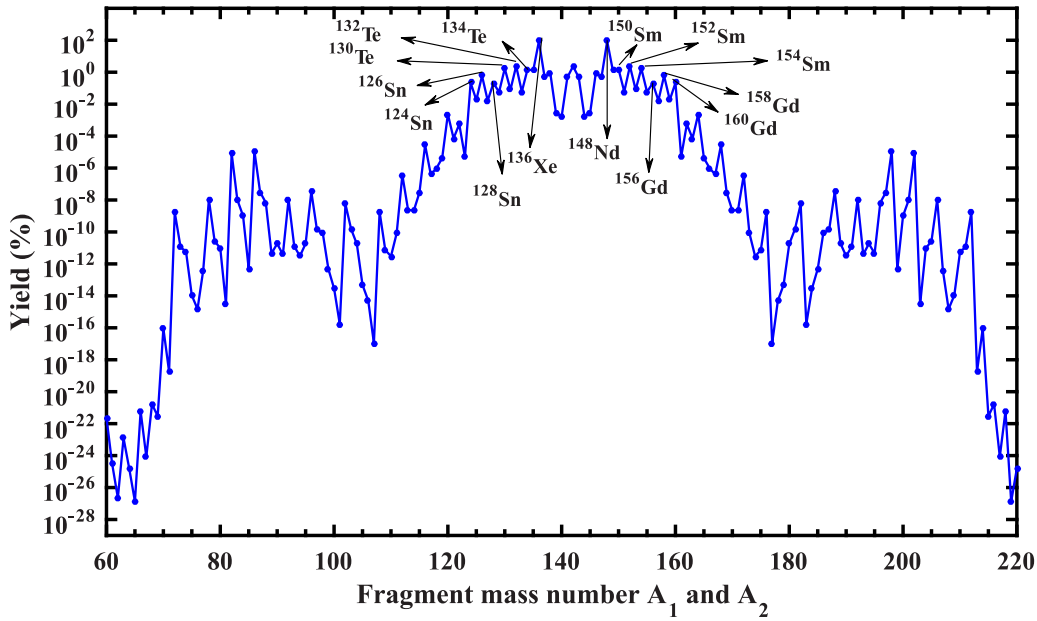

FIG. 5. Relative yields of all possible even fragmentations for ^{284}Fl superheavy isotope as a function of fragments mass number (A_1 and A_2). Favored fragment combinations with higher yield are labeled.

$[\lambda = \lambda_1 + \lambda_2 + \cdots + \lambda_n)]$. Then half-life of the spontaneous fission for ^{284}Cn and ^{284}Fl are evaluated using Eq. (9). The results of the present model for ^{284}Cn and ^{284}Fl superheavy nuclei are presented in Tables III and IV, respectively. Amounts 0.33 ms and 0.148 ms are obtained for spontaneous fission half-lives of ^{284}Cn and ^{284}Fl superheavy nuclei, respectively.

IV. CALCULATION OF SPONTANEOUS FISSION HALF-LIFE USING SEMIEMPIRICAL FORMULAS

Ren and his coworkers [65] calculated half-life of spontaneous fission of superheavy nuclei using the following

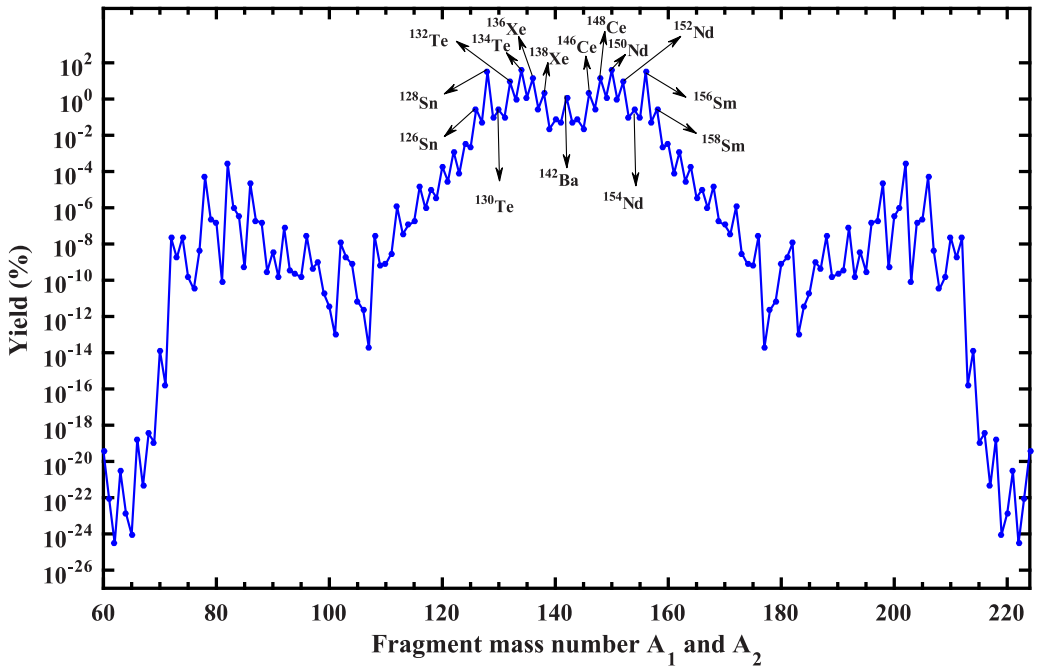

FIG. 6. Relative yields of all possible even fragmentations for ^{284}Cn superheavy isotope as a function of fragments mass number (A_1 and A_2). Favored fragment combinations with higher yield are labeled.

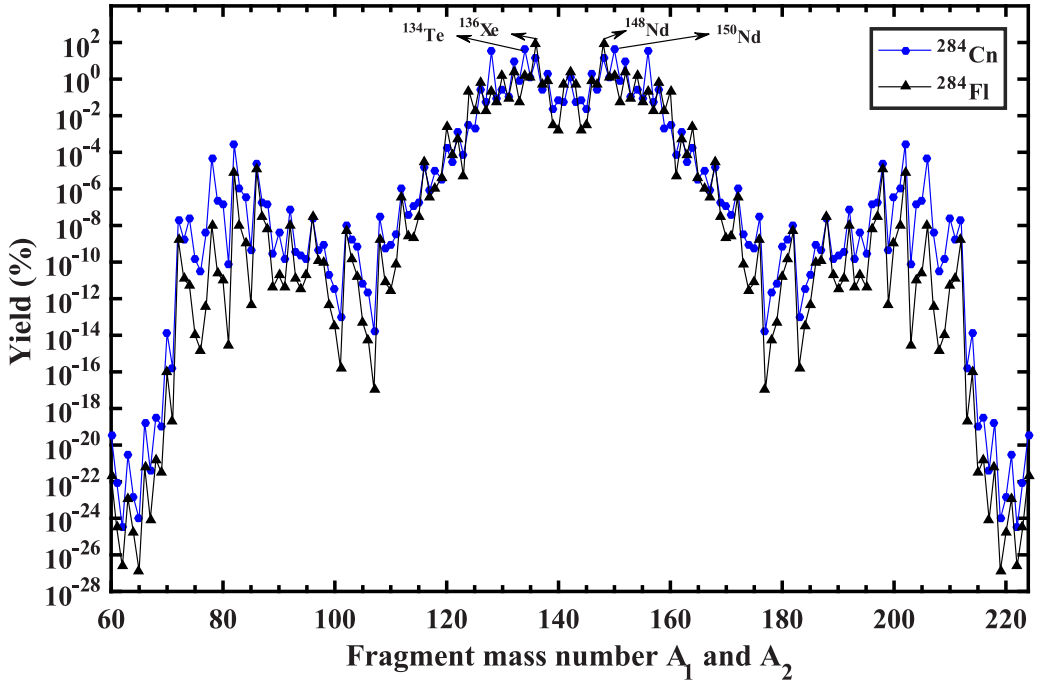

FIG. 7. Relative yields of all possible even fragmentations for ^{284}Fl and ^{284}Cn superheavy isobars as a function of fragments mass number(A_1 and A_2) are compared. Favored fragment combinations with the highest yield is labeled.

semiempirical formula:

$$\log_{10}T_{1/2} = 21.08 + c_1\frac{(Z-90-\nu)}{A} + c_2\frac{(Z-90-\nu)^2}{A} + c_3\frac{(Z-90-\nu)^3}{A} + c_4\frac{(Z-90-\nu)(N-Z-52)^2}{A}, \quad (12)$$

where, c_1, c_2, c_3, and c_4 are adjusting parameters that can be evaluated using experimental data and ν is the number of prompt neutrons emitted in spontaneous fission. Also, A and Z are mass and atomic numbers of fissioning nucleus. Xu and his research group [66] presented the following semiempirical formula to estimate the spontaneous fission half-life

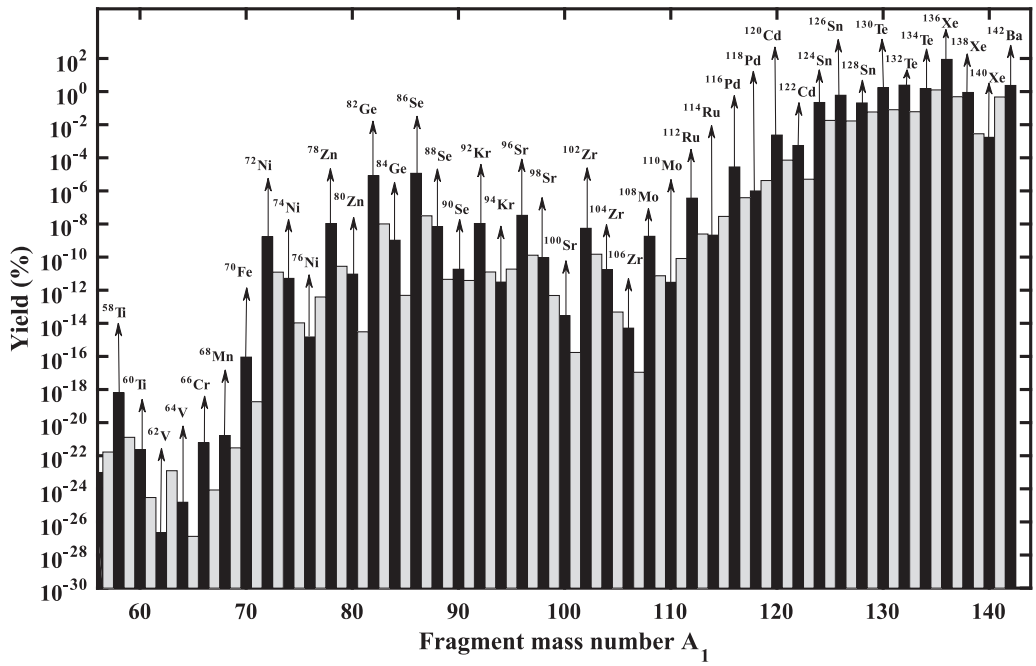

FIG. 8. Bar graph presentation of relative yields for spontaneous even and odd fragmentations of ^{284}Fl superheavy nucleus.

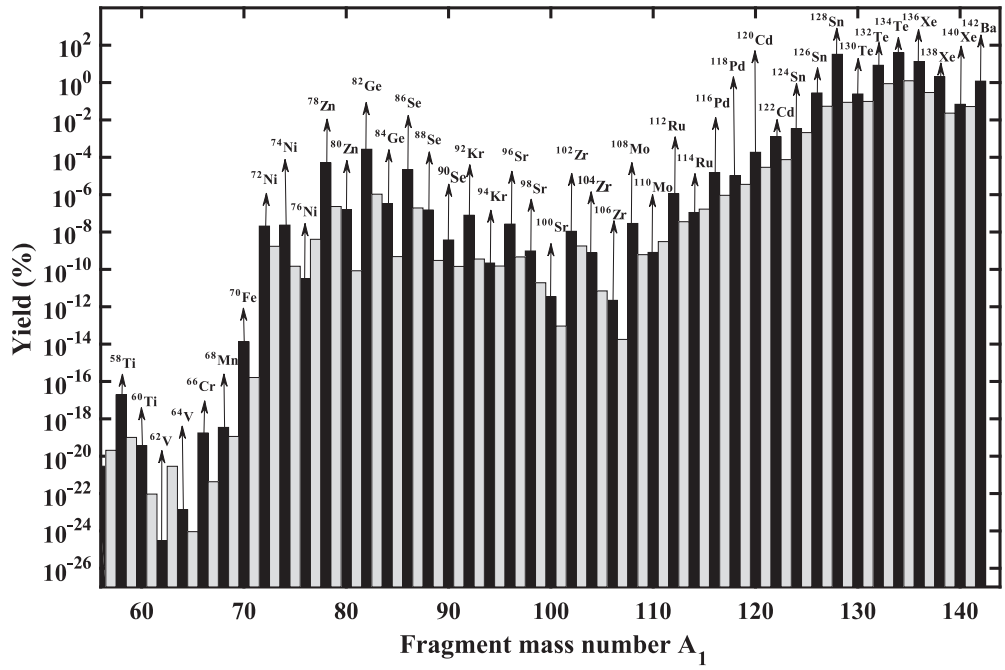

FIG. 9. Bar graph presentation of relative yields for spontaneous even and odd fragmentations of ^{284}Cn superheavy nucleus.

of superheavy nuclei:

$$\log_{10}T_{1/2} = 2\pi\left[C_0 + C_1A + C_2Z^2 + C_3Z^4 + C_4(N-Z)^2 - \left(0.13323\frac{Z^2}{Z^{1/3}} - 11.64\right)\right], \quad (13)$$

where, C_0, C_1, C_2, C_3, and C_4 are constants that adjusted using experimental data. The following semiempirical relation is employed by Karpov and his collaborators [67] to calculate half-life of superheavy nuclei:

$$\log_{10}T_{1/2} = 1146.44 - 75.3153(Z^2/A) + 1.63792(Z^2/A)^2 - 0.0119827(Z^2/A)^3 + B_f(7.23613 - 0.0947022Z^2/A) + h, \quad (14)$$

where B_f is the fission barrier and can be calculated using the liquid drop model (LDM) and h is a constant ($h = 0$ for even A and Z, $h = 1.53897$ for odd A, and $h = 0.80822$ for odd A and Z). Finally, Santhosh and his coauthors [68] estimated the spontaneous fission half-life of superheavy nuclei using the

TABLE III. Spontaneous fission constant, λ_i (s^{-1}), for each individual fragmentation of ^{284}Fl superheavy nucleus (λ_i's less than 10^{-7} are neglected).

A_1	A_2	λ_i (s^{-1})	A_1	A_2	λ_i (s^{-1})	A_1	A_2	λ_i (s^{-1})
^{4}He	^{280}Cn	2.78011	^{92}Kr	^{192}Pt	0.0000032	^{126}Sn	^{158}Gd	209.7591
^{8}Be	^{276}Ds	1.01212	^{96}Sr	^{188}Os	0.0000101	^{127}Sn	^{157}Gd	5.849377
^{9}Be	^{275}Ds	0.01017	^{102}Zr	^{182}W	0.0000017	^{128}Sn	^{156}Gd	71.75805
^{10}Be	^{274}Ds	0.00885	^{108}Mo	^{176}Hf	0.0000006	^{129}Sb	^{155}Eu	20.53673
^{11}Be	^{273}Ds	0.000025	^{112}Ru	^{172}Yb	0.000119	^{130}Te	^{154}Sm	604.0533
^{12}Be	^{272}Ds	0.000001	^{113}Ru	^{171}Yb	0.0000008	^{131}Te	^{153}Sm	28.2163
^{13}B	^{271}Mt	0.000003	^{114}Ru	^{170}Yb	0.0000007	^{132}Te	^{152}Sm	861.1417
^{14}C	^{270}Hs	0.000523	^{115}Rh	^{169}Tm	0.0000094	^{133}Te	^{151}Sm	21.2937
^{15}C	^{269}Hs	0.000002	^{116}Pd	^{168}Er	0.009317	^{134}Te	^{150}Sm	540.4294
^{16}C	^{268}Hs	0.0000002	^{117}Pd	^{167}Er	0.000129	^{135}I	^{149}Pm	445.272
^{72}Ni	^{212}Rn	0.0000004	^{118}Pd	^{166}Er	0.000329	^{136}Xe	^{148}Nd	313.63
^{78}Zn	^{206}Po	0.000003	^{119}Ag	^{165}Ho	0.001424	^{137}Xe	^{147}Nd	173.0164
^{82}Ge	^{202}Pb	0.002295	^{120}Cd	^{164}Dy	0.806454	^{138}Xe	^{146}Nd	313.5251
^{83}Ge	^{201}Pb	0.0000028	^{121}Cd	^{163}Dy	0.024551	^{139}Xe	^{145}Nd	0.988355
^{84}Ge	^{200}pb	0.0000003	^{122}Cd	^{162}Dy	0.18879	^{140}Xe	^{144}Nd	0.60399
^{86}Se	^{198}Hg	0.003344	^{123}Cd	^{161}Dy	0.001715	^{141}Ba	^{143}Ce	167.4358
^{87}Se	^{197}Hg	0.000009	^{124}Sn	^{160}Gd	76.79021	^{142}Ba	^{142}Ce	835.6867
^{88}Se	^{196}Hg	0.000002	^{125}Sn	^{159}Gd	6.30164			

TABLE IV. Spontaneous fission constant, λ_i (s^{-1}), for each individual fragmentation of ^{284}Cn superheavy nucleus (λ_i's less than 10^{-7} are neglected).

A_1	A_2	λ_i (s^{-1})	A_1	A_2	λ_i (s^{-1})	A_1	A_2	λ_i (s^{-1})
^{4}He	^{280}Ds	2.59	^{88}Se	^{196}Pt	1.8×10^{-5}	^{123}Cd	^{161}Gd	0.010537
^{8}Be	^{276}Hs	0.416393	^{90}Se	^{194}Pt	4.39×10^{-7}	^{124}Sn	^{160}Sm	0.474318
^{9}Be	^{275}Hs	0.006343	^{92}Kr	^{192}Os	9.71×10^{-6}	^{125}Sn	^{159}Sm	0.299547
^{10}Be	^{274}Hs	0.009415	^{96}Sr	^{188}W	3.34×10^{-6}	^{126}Sn	^{158}Sm	39.95672
^{11}Be	^{273}Hs	4.55×10^{-5}	^{98}Sr	^{186}W	1.2×10^{-7}	^{127}Sn	^{157}Sm	7.746259
^{12}Be	^{272}Hs	3.63×10^{-6}	^{102}Zr	^{182}Hf	1.4×10^{-6}	^{128}Sn	^{156}Sm	470.2821
^{13}B	^{271}Bh	2.38×10^{-6}	^{103}Zr	^{181}Hf	2.29×10^{-7}	^{129}Sb	^{155}Pm	12.62111
^{14}C	^{270}Sg	0.000162	^{108}Mo	^{176}Yb	3.78×10^{-6}	^{130}Te	^{154}Nd	35.33992
^{15}C	^{269}Sg	1.65×10^{-6}	^{110}Mo	^{174}Yb	1.05×10^{-7}	^{131}Te	^{153}Nd	14.1451
^{72}Ni	^{212}Po	2.16×10^{-6}	^{111}Tc	^{173}Tm	4.06×10^{-7}	^{132}Te	^{152}Nd	12.28068
^{73}Ni	^{211}Po	1.78×10^{-7}	^{112}Ru	^{172}Er	0.000149	^{133}Te	^{151}Nd	17.72009
^{74}Ni	^{210}Po	2.44×10^{-6}	^{113}Ru	^{171}Er	4.78×10^{-6}	^{134}Te	^{150}Nd	572.3825
^{77}Cu	^{207}Bi	4.32×10^{-6}	^{114}Ru	^{170}Er	1.5×10^{-5}	^{135}I	^{149}Pr	182.8811
^{78}Zn	^{206}Pb	0.005633	^{115}Rh	^{169}Ho	2.28×10^{-5}	^{136}Xe	^{148}Ce	196.9272
^{79}Zn	^{205}Pb	2.55×10^{-5}	^{116}Pd	^{168}Dy	0.002099	^{137}Xe	^{147}Ce	42.86341
^{80}Zn	^{204}Pb	1.69×10^{-5}	^{117}Pd	^{167}Dy	0.000127	^{138}Xe	^{146}Ce	295.0016
^{82}Ge	^{202}Hg	0.031534	^{118}Pd	^{166}Dy	0.001417	^{139}Xe	^{145}Ce	3.340531
^{83}Ge	^{201}Hg	0.000122	^{119}Ag	^{165}Tb	0.000492	^{140}Xe	^{144}Ce	9.955773
^{84}Ge	^{200}Hg	3.82×10^{-5}	^{120}Cd	^{164}Gd	0.026045	^{141}Ba	^{143}Ba	7.562873
^{86}Se	^{198}Pt	0.002622	^{121}Cd	^{163}Gd	0.004076	^{142}Ba	^{142}Ba	174.3454
^{87}Se	^{197}Pt	2.32×10^{-5}	^{122}Cd	^{162}Gd	0.176633			

following semiempirical formula:

$$\log_{10} T_{1/2} = \mathrm{a}(Z^2/A) + b(Z^2/A)^2 + c\left(\frac{N-Z}{N+Z}\right) + d\left(\frac{N-Z}{N+Z}\right)^2 + e, \quad (15)$$

where a, b, c, d, and e are coefficients that evaluated by fitting with experimental data. In addition to direct calculation, the spontaneous fission logarithmic half-life of ^{284}Cn and ^{284}Fl superheavy nuclei are evaluated using presented semiempirical methods to examine results of direct method. Obtained half-lifes for ^{284}Cn and ^{284}Fl superheavy nuclei using the direct method are compared with the results of semiempirical approaches as well as experimental data in Table V.

V. CONCLUSION

In the present investigation, the spontaneous binary cold fission of ^{284}Fl and ^{284}Cn superheavy isobars are studied. For each individual fragmentation, Q value and driving potential ($V - Q$) are calculated considering the Coulomb and the nuclear proximity potentials. The tunneling probability, fission decay constant, and relative yield are obtained as well for each possible fragments combinations. Obtained results indicate that the relative yield for production of the even mass fragment is more probable than the odd mass ones. The shell effects played major role in spontaneous fission of superheavy nuclei. Analysis of obtained results clearly show that production of double magic, magic, and closed-shell fragments are more probable than other combinations of fragments. In this regard, due to the presence of ^{136}Xe with neutron magic shell ($N = 82$) isotope, the fragmentation ^{136}Xe + ^{148}Nd for ^{284}Fl superheavy isotope and production of magic ^{134}Te isotope with ($N = 82$) neutron magic shell, the fragment combination ^{134}Te + ^{150}Nd for spontaneous fission of ^{284}Cn happens with the highest probability. Fission decay constant, λ_i, for each individual fragmentation is obtained and total fission decay constant is also evaluated by summing over decay constants of all possible fragmentation. Finally, the spontaneous fission half-life of ^{284}Fl and ^{284}Cn isobars are evaluated. However, the logarithmic half-life of ^{284}Fl and ^{284}Cn isobars are evaluated using presented semiempirical approaches. Calculated logarithmic half-life using direct and semiempirical methods are compared with experimental data in Table V. As it is clear from this table, our obtained half-life using direct method are better agreed with experimental data than the results of semiempirical methods.

TABLE V. The evaluated logarithmic spontaneous fission half-lives (in seconds) of ^{284}Cn and ^{284}Fl superheavy nuclei using the direct method are compared with the results of various semiempirical approaches as well as experimental data.

Parent nucleus	Semiempirical [65]	Semiemperical [66]	Semiempirical [67]	Semiempirical [68]	(Direct method)	(Expt. [62,64])
^{284}Cn	−15.53	−3.93	5.34	−3.98	−3.48	−1.001
^{284}Fl	2.89	1.68	5.07	−0.32	−3.83	−2.602

[1] M. R. Pahlavani and S. M. Mirfathi, Eur. Phys. J. A **52**, 95 (2016).
[2] M. R. Pahlavani and S. M. Mirfathi, Phys. Rev. C **92**, 024622 (2015).
[3] M. R. Pahlavani and P. Mehdipour, Int. J. Mod. Phys. E **27**, 1850018 (2018).
[4] A. Deppman, E. Andrade-II, V. Guimarães, G. S. Karapetyan, and N. A. Demekhina, Phys. Rev. C **87**, 054604 (2013).
[5] D. H. Morse, A. J. Antolak, and B. L. Doyle, Nucl. Inst. Metho. Phys. Res. B **261**, 378 (2007).
[6] Y. Ayyad, J. Benlliure *et al.*, Phys. Rev. C **89**, 054610 (2014).
[7] K. B. Gikal, E. M. Kozulin, A. A. Bogacher *et al.*, Phys. Atom. **79**, 1367 (2016).
[8] D. Naderi, M. R. Pahlavani, and S. A. Alavi, Phys. Rev. C **87**, 054618 (2013).
[9] M. R. Pahlavani and D. Naderi, Eur. Phys. J. A **48**, 129 (2012).
[10] M. R. Pahlavani, D. Naderi, and S. M. Mirfathi, Mod. Phys. Lett. A **26**, 1323 (2011).
[11] P. B. Price, Nucl. Phys. A **502**, 41 (1989).
[12] O. Hahn and F. Strassmann, Naturwissenschaften **27**, 11 (1939).
[13] L. Meitner and O. R. Frisch, Nature **143**, 239 (1939).
[14] O. R. Frisch, Nature **143**, 276 (1939).
[15] N. Bohr and J. A. Wheeler, Phys. Rev. **56**, 426 (1939).
[16] M. R. Pahlavani and S. M. Mirfathi, Phys. Rev. C **96**, 014606 (2017).
[17] M. R. Pahlavani and S. M. Mirfathi, Phys. Rev. C **93**, 044617 (2016).
[18] M. R. Pahlavani and D. Naderi, Phys. Rev. C **83**, 024602 (2011).
[19] K. Nishio *et al.*, Phys. Rev. C **82**, 044604 (2010).
[20] D. J. Hinde, R. du Rietz, M. Dasgupta, R. G. Thomas, and L. R. Gasques, Phys. Rev. Lett. **101**, 092701 (2008).
[21] C. Signarbieux, M. Montoya, M. Ribrag, C. Mazur, C. Guet, P. Perrin, and M. Maurel, J. Phys. Lett. **42**, 437 (1981).
[22] P. Armbruster *et al.*, in *Proceeding of 4th International Conference on Nuclei Far from Stability*, Helsingør, Denmark, 7 - 13 Jun 1981 (CERN-1981-009), pp. 675–679.
[23] F. J. Hambsch, H. H. Knitter, and C. B. Jorgensen, Nucl. Phys. A **554**, 209 (1993).
[24] W. Schwab, H. G. Clerc, M. Mutterer, J. P. Theobald, and H. Faust, Nucl. Phys. A **577**, 674 (1994).
[25] A. Benoufella, G. Barreau, M. Asghar, P. Audouard, F. Brisard, T. P. Doan, M. Hussonnois, B. Leroux, J. Trochon, and M. S. Moore, Nucl. Phys. A **565**, 563 (1993).
[26] M. Warda and L. M. Robledo, Phys. Rev. C **84**, 044608 (2011).
[27] J. H. Hamilton, A. V. Ramayya, J. Kormicki, W. C. Ma, Q. Lu, D. Shi, J. K. Deng, S. J. Zhu, A. Sandulescu, W. Greiner, G. M. Ter-Akopian, Y. T. Oganessian, G. S. Popeko, A. V. Daniel, J. Kliman, V. Polhorsky, M. Morhac, J. D. Cole, R. Aryaeinejad, I. Y. Lee, N. R. Johnson, and F. K. McGowan, J. Phys. G **20**, L85 (1994).
[28] G. M. Ter-Akopian, J. H. Hamilton, Y. T. Oganessian, J. Kormicki, G. S. Popeko, A. V. Daniel, A. V. Ramayya, Q. Lu, K. Butler-Moore, W. C. Ma, J. K. Deng, D. Shi, J. Kliman, V. Polhorsky, M. Morhac, W. Greiner, A. Sandelescu, J. D. Cole, R. Aryaeinejad, N. R. Johnson, I. Y. Lee, and F. K. McGowan, Phys. Rev. Lett. **73**, 1477 (1994).
[29] A. Sandulescu and W. Greiner, J. Phys. G **3**, L189 (1977).
[30] A. Sandulescu and W. Greiner, Rep. Prog. Phys. **55**, 1423 (1992).
[31] A. Sandulescu, A. Florescu, F. Carstoiu, W. Greiner, J. H. Hamilton, A. V. Ramayya, and B. R. S. Babu, Phys. Rev. C **54**, 258 (1996).
[32] Y. X. Dardenne, R. Aryaeinejad, S. J. Asztalos, B. R. S. Babu, K. Butler-Moore, S. Y. Chu, J. D. Cole, M. W. Drigert, K. E. Gregorich, J. H. Hamilton, J. Kormicki, I. Y. Lee, R. W. Lougheed, Q. H. Lu, W. C. Ma, M. F. Mohar, K. J. Moody, S. G. Prussin, A. V. Ramayya, J. O. Rasmussen, M. A. Stoyer, and J. F. Wild, Phys. Rev. C **54**, 206 (1996).
[33] S. Kumar and R. K. Gupta, Phys. Rev. C **49**, 1922 (1994).
[34] F. Gonnenwein, A. Moller, M. Cronni, M. Hesse, M. Wostheinrich, H. Faust, G. Fioni, and S. Oberstedt, Nuovo Cimento A **110**, 1089 (1997).
[35] E. R. Hulet, J. F. Wild, R. J. Dougan, R. W. Lougheed *et al.*, Phys. Rev. Lett. **56**, 313 (1986).
[36] A. V. Ramayya, J. H. Hamilton, J. K. Hwang, L. K. Peker *et al.*, Phys. Rev. C **57**, 2370 (1998).
[37] R. Smolanczuk, Phys. Rev. C **56**, 812 (1997).
[38] J. H. Hamilton, S. Hofmann, and Y. T. Oganessian, Annu. Rev. Nucl. Part. Sci. **63**, 383 (2013).
[39] A. Tamii, I. Poltoratska, P. Von Neumann-Cosel, Y. Fujita *et al.*, Phys. Rev. Lett. **107**, 062502 (2011).
[40] J. Khuyagbaatar, A. Yakushev, Ch. E. Dullmann, D. Ackermann *et al.*, Phys. Rev. Lett. **112**, 172501 (2014).
[41] K. Morita, K. Morimoto, D. Kaji *et al.*, J. Phys. Soc. Jpn. **76**, 045001 (2007).
[42] Yu. Oganessian, Radiochimica. Acta **99**, 429 (2011).
[43] A. Staszczak, A. Baran, and W. Nazarewicz, Phys. Rev. C **87**, 024320 (2013).
[44] D. N. Poenaru and R. A. Gherghescu, J. Phys. G: Nucl. Part. Phys. **41**, 125104 (2014).
[45] D. C. Hoffman, T. M. Hamilton, and M. R. Lane, in *Nuclear Decay Modes*, edited by D. N. Poenaru (Institute of Physics Publishing IOP, Bristol, 1996), pp. 393–432, chap. 10.
[46] M. R. Pahlavani, O. N. Ghodsi, and M. Zadehrafi, Phys. Rev. C **96**, 054612 (2017).
[47] M. R. Pahlavani and M. Joharifard, Eur. Phys. J. A **54**, 171 (2018).
[48] K. P. Santhosh, R. K. Biju, and S. Sabina, J. Phys. G: Nucl. Part. Phys. **36**, 115101 (2009).
[49] M. Brack, Jens Damgaard, A. S. Jensen, H. C. Pauli, V. M. Strutinsky, and C. Y. Wong, Rev. Mod. Phys. **44**, 320 (1972).
[50] D. N. Poenaru and R. A. Gherghescu, Phys. Rev. C **94**, 014309 (2016).
[51] D. N. Poenaru and R. A. Gherghescu, Europhys. Lett. **118**, 22001 (2017).
[52] S. Hofmann *et al.*, in *Proceedings of the 6th International Conference on ICFN6, Sanibel Island, Florida, USA, 2016*, edited by J. H. Hamilton, A. V. Ramayya, and P. Talou (World Scientific, Singapore, 2018), pp. 88–100.
[53] K. P. Santhosh and B. Priyanka, Nucl. Phys. A **940**, 21 (2015).
[54] A. C. Wahl, At. Data Nucl. Data Tables **39**, 1 (1988).
[55] J. Blocki, J. Randrup, W. J. Swiatecki, and C. F. Tsang, Ann. Phys. NY **105**, 427 (1977).
[56] J. Blocki and W. J. Swiatecki, Ann. Phys. NY **132**, 53 (1981).
[57] C. L. Guo, G. L. Zhang, and X. Y. Le, Nucl. Phys. A **897**, 54 (2013).

[58] D. N. Poenaru, M. Ivascu, A. Sandulescu, and W. Greiner, Phys. Rev. C **32**, 572 (1985).
[59] G. Audi and A. H. Wapstra, Nucl. Phys. A **595**, 409 (1995).
[60] G. Audi, F. G. Kondev, M. Wang, B. Pefeiffer, X. Sun, J. Blachot, and M. MacCormick, Chin. Phys. C **36**, 1157 (2012).
[61] A. H. Wapstra, G. Audi, and C. Thibault, Nucl. Phys. A **729**, 129 (2003).
[62] G. Audi *et al.*, Chin. Phys. C **41**, 030001 (2017).
[63] D. N. Poenaru, W. Greiner, and R. A. Gherghescu, Atom. Data Nucl. Data Tables **68**, 91 (1998).
[64] V. K. Utyonkov, N. T. Brewer, Yu. Ts. Oganessian *et al.*, Phys. Rev. C **92**, 034609 (2015).
[65] Z. Ren and C. Xu, Nucl. Phys. A **759**, 64 (2005).
[66] Ch. Xu, Zh. Ren, and Y. Guo, Phys. Rev. C **78**, 044329 (2008).
[67] A. V. Karpov, V. I. Zagrebaev, W. Greiner, L. F. Ruiz, and Y. M. Palenzuela, Int. J. Mod. Phys. E **21**, 1250013 (2012).
[68] K. P. Santhosh, R. K. Biju, and S. Sabina, Nucl. Phys. A **832**, 220 (2010).